Millisecond Measurement of Transport During and After an Electroporation Pulse

Mark R. Prausnitz,* James D. Corbett,‡§ J. Aura Gimm,*¶ David E. Golan,‡§ Robert Langer,*¶ and James C. Weaver¶

*Department of Chemical Engineering, Massachusetts Institute of Technology, Cambridge, Massachusetts 02139, ‡Departments of Biological Chemistry and Molecular Pharmacology and Medicine, Harvard Medical School, Boston, Massachusetts 02115, §Division of Hematology/Oncology, Brigham and Women's Hospital, Boston, Massachusetts 02115, and ¶Harvard/MIT Division of Health Sciences and Technology, Massachusetts Institute of Technology, Cambridge, Massachusetts 02139 USA

ABSTRACT Electroporation involves the application of an electric field pulse that creates transient aqueous pathways in lipid bilayer membranes. Transport through these pathways can occur by different mechanisms during and after a pulse. To determine the time scale of transport and the mechanism(s) by which it occurs, efflux of a fluorescent molecule, calcein, across erythrocyte ghost membranes was measured with a fluorescence microscope photometer with millisecond time resolution during and after electroporation pulses several milliseconds in duration. One of four outcomes was typically observed. Ghosts were: (1) partially emptied of calcein, involving efflux primarily after the pulse; (2) completely emptied of calcein, involving efflux primarily after the pulse; (3) completely emptied of calcein, involving efflux both during and after the pulse; or (4) completely emptied of calcein, involving efflux primarily during the pulse. Partial emptying, involving significant efflux during the pulse, was generally not observed. We conclude that under some conditions transport caused by electroporation occurs predominantly by electrophoresis and/or electroosmosis during a pulse, although under other conditions transport occurs in part or almost completely by diffusion within milliseconds to seconds after a pulse.

INTRODUCTION

Electroporation involves the creation of transient aqueous pathways in lipid bilayer membranes by the application of a short (micro- to millisecond) electric field pulse (Neumann et al., 1989; Tsong, 1991; Chang et al., 1992; Orlowski and Mir, 1993; Weaver, 1993). Electroporation increases permeability and electrical conductance of both cell membranes and artificial lipid bilayers by orders of magnitude. Membrane changes can be reversible or irreversible, depending mainly on pulse magnitude and duration. Electrical exposures typically involve electric field pulses that generate transmembrane potentials of approximately 1 V and last for 10 μs to 10 ms (Neumann et al., 1989; Chang et al., 1992).

Electropores are thought to be created on the submicrosecond time scale (Kinosita and Tsong, 1977b; Benz et al., 1979; Hibino et al., 1991; Neumann et al., 1992) and to continue growing in size for the duration of the electrical exposure (Kinosita and Tsong, 1977a; Barnett and Weaver, 1991; Freeman et al., 1994). After the pulse, pores are believed to shrink to a metastable state over a characteristic time of milliseconds (Chernomordik et al., 1983; Glaser et al., 1988) and, under reversible conditions, to disappear completely over lifetimes ranging from sub-second to hours (Zimmermann et al., 1975; Abidor et al., 1979; Chang and Reese, 1990; Hibino et al., 1991; Zhelev and Needham, 1993).

Transport caused by electroporation is expected to occur by different mechanisms at different times. During a pulse, transport could occur by diffusion and/or electrically driven transport (e.g., electrical drift and electroosmosis) through electropores. After a pulse, transport could occur through electropores, as long as pores exist, by diffusion and/or low voltage electrically driven transport caused by a small transmembrane diffusion potential (Weaver and Barnett, 1992).

Although a number of studies have shown that molecular transport through electropores can occur seconds to hours after a pulse (Mishra and Singh, 1986; Lambert et al., 1990; Rols and Teissié, 1990; Tekle et al., 1991; Lee et al., 1992), it has been proposed that most transport occurs during a pulse, driven by electrical drift or electroosmosis (Dimitrov and Sowers, 1990; Klenchin et al., 1991; Weaver and Barnett, 1992; Orlowski and Mir, 1993; Prausnitz et al., 1994). However, the kinetics of transport caused by electroporation have not been measured on a time scale as fast or faster than that of the pulse, making it difficult to compare transport rates during and after the pulse. Such information could give direct insight into transport mechanisms. This lack motivated the following study, in which molecular efflux across erythrocyte ghost membranes was measured on the millisecond time scale during and after electroporation pulses several milliseconds in duration.

Received for publication 15 July 1994 and in final form 10 February 1995.

Address reprint requests to Dr. Robert Langer, Harvard/MIT Division of Health Sciences and Technology, Massachusetts Institute of Technology, Cambridge, MA 02115.

Dr. Prausnitz' present address: School of Chemical Engineering, Georgia Institute of Technology, Atlanta, GA 30332.

Dr. Corbett's present address: Department of Laboratory Medicine, University of California, San Francisco, San Francisco CA 94143.

0006-3495/95/05/1864/07 $2.00

MATERIALS AND METHODS

Erythrocyte ghost preparation

Erythrocyte membranes are commonly used in electroporation studies (Sale and Hamilton, 1968; Zimmermann et al., 1976; Kinosita and Tsong, 1977a; Chang and Reese, 1990; Dimitrov and Sowers, 1990; Prausnitz et al., 1993). The preparation of erythrocyte ghosts and the loading of ghosts with fluorescent molecules have been described previously (Prausnitz et al., 1993). Briefly, human erythrocytes were washed and lysed by hypotonic shock. Calcein (Molecular Probes, Eugene, OR) was loaded into the ghosts before resealing by exposure to a solution of 1 mM calcein. Loaded ghosts were stored as a pellet at 4°C for up to 1 day and washed again before use.

Pulsing chamber design

The pulsing chamber is shown in Fig. 1. Microscope slides were adhered to one another with silicone rubber (RTV silicone rubber, General Electric Co., Waterford, NY) to make a mounting stand that provided mechanical stability and electrical insulation from the metal microscope stage. Two stainless steel electrodes (4 × 1 × 0.2 mm, with polished surfaces and 90° corners) were affixed with silicone rubber in parallel to the mounting stand, with an interelectrode spacing of 1.6 mm. The electrodes were further polished with emery cloth until the top surfaces were flat and co-planar. An enclosed trough (the experimental chamber) was made by filling the outer edges of the interelectrode spaces with silicone rubber.

Electroporation protocol

Calcein-loaded erythrocyte ghosts were immobilized on one side of a glass coverslip (16 × 16 mm) coated with Cell-Tak cell adhesive (20–180 min adhesion time; Becton Dickinson Labware, Bedford, MA). The experimental chamber was filled with phosphate-buffered saline (pH 7.4, 1.1 g/L NaCl, 0.15 g/L Na_2HPO_4, 0.027 g/L KCl, 0.027 g/L KH_2PO_4 (Prausnitz et al., 1993)). The coverslip was then placed on top of the chamber so that the ghost-coated surface was facing down, bathed in saline. A small drop of silicone grease (high vacuum grease, Dow Corning Corp., Midland, MI) was placed over one or two corners of the coverslip to prevent it from moving. The chamber was positioned on the stage of the fluorescence microscope photometer (see below) so that a single immobilized and isolated ghost was illuminated by the excitation beam. A laser beam 5 μm in radius, slightly larger than a ghost, was used to assure that the ghost remained within the excitation beam even if the ghost moved or deformed slightly during the electroporation pulse. After waiting 1 to 2 min to verify that the ghost was well anchored, an exponential decay electric field pulse was applied across the chamber with a capacitor discharge power supply (Gene Pulser, Bio-Rad Laboratories, Richmond, CA). The electric field strength was varied from 1.0 to 3.8 kV/cm. The exponential decay time constant, τ, was 3.6 ± 1.1 ms (mean ± standard deviation). The internal signal that triggered the pulse output from the power supply was also used to initiate data collection.

Ghost immobilization was required to assure that the ghost remained within the excitation beam throughout the experiment. Unlike electroporation of cells in suspension, electroporation of ghosts immobilized to a charged surface (i.e., Cell-Tak-coated glass) may cause additional shear forces caused by (1) differential movement of immobilized and free portions of the ghost membrane caused by electrophoresis and (2) hydrodynamic shear caused by electroosmosis at the charged surface.

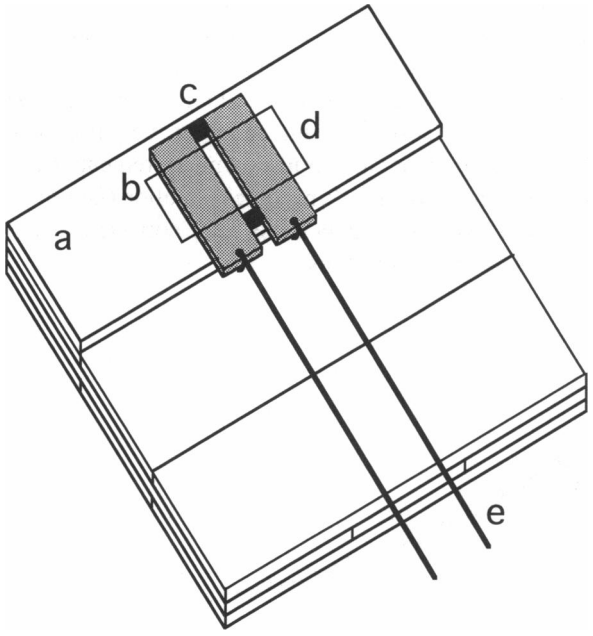

FIGURE 1 Pulsing chamber design. A mounting stand (*a*) provided a platform for two parallel, co-planar stainless steel electrodes (*b*). To form an enclosed trough, the interelectrode spaces on the outer edges were filled with silicone rubber (*c*). A coverslip (*d*) coated on its underside with immobilized erythrocyte ghosts was placed on top. This design allowed measurement of ghost fluorescence with a fluorescence microscope photometer during and after electroporation.

Fluorescence measurements

Fluorescence emission from a single calcein-loaded ghost was quantified with an instrument modified from a time-resolved fluorescence microscope photometer described previously (Corbett and Golan, 1993). The light source for fluorescence excitation was a 5-W argon ion laser (Spectra-Physics 164–08, Mountain View, CA) tuned to 488 nm. Intensity modulation by an acoustooptic modulator (Newport Electro-Optics N35083–3, Melbourne, FL) provided the two light intensities required for (1) locating cells (low intensity) and (2) following changes in fluorescence after the application of an electric field pulse (high intensity). The high intensity beam did not cause significant photobleaching of calcein over the 0.02–10 s experimental period. Before entering a fluorescence microscope (Leitz Orthoplan/MPV-3, Rockleigh, NJ), the intensity-modulated light was passed through a 500-mm biconvex lens (Ealing Corp., Natick, MA). This beam was directed onto the microscope stage by a 515-nm dichroic (Leitz) and focused at the sample plane by an adjustable short focal length lens within the body of the microscope and by a strain-free 40× 0.65 numerical aperature air objective. Experiments were performed at room temperature (~23°C).

Fluorescence emission was collected from the sample by the microscope objective and filtered by the dichroic and a 520-nm long pass filter. Emitted light was detected by a single-photon counting system consisting of a thermionically cooled (Products for Research TE-104RF, Danvers, MA) photomultiplier tube (PMT; Thorn EMI 9658RA, Fairfield, NJ) driven by a high voltage power supply (EG&G 1109, Princeton, NJ). An adjustable field diaphragm was used to discriminate against fluorescence from regions other than the ghost of interest. PMT pulses were amplified and discriminated to 100 mV (EG&G 1121A). The resulting transistor-transistor logic pulses were fed into a multichannel scaler (Nicolet 370, Madison, WI), triggered by the pulsing unit to initiate data collection at the beginning of the electric field pulse (time = 0). Fluorescence values were normalized to the fluorescence of the ghosts before application of the electric field pulse. After each experiment, data were transferred to a computer workstation (Sun 386i/250, Mountain View, CA) for processing.

As a result of background fluorescence and noise, the fluorescence of a ghost completely emptied of calcein was not zero. Because the level of background was a function of the data collection rate, local ghost density, degree of efflux from neighboring ghosts, and other factors, we could not reliably subtract it from our measurements. All reported fluorescence values therefore contained background fluorescence. In this report we have interpreted those cases in which fluorescence reached a very low (typically, normalized fluorescence < 0.1) and unchanging value as complete emptying of calcein from a ghost.

Electric field validation

Because ghosts immobilized on coverslips were located slightly above the plane of the electrodes, the local electric field was slightly less than the nominal electric field between the electrodes. Using the microscope, we determined that ghosts were at most 100 μm above the plane of the upper surfaces of the electrodes. Numerically solving by finite element analysis (Maxwell 2D Field Simulator, Ansoft Corp., Pittsburgh, PA) for the field in the chamber with the geometry of our apparatus, the electric field experienced by the ghosts was estimated to be within 1% of the nominal electric field.

RESULTS

Erythrocyte ghosts were loaded with calcein, a small (M_r = 623), highly charged (z = −4), fluorescent molecule that is unable to cross resealed erythrocyte ghost membranes. The fluorescence of individual calcein-loaded ghosts was measured during and after single exponential decay (τ = 3.6 ± 1.1 ms) electric field pulses. Rates and time scales of calcein efflux across ghost membranes were assessed with millisecond temporal resolution. Data were normalized to prepulse fluorescence values determined before pulsing. To assure that no photobleaching of calcein occurred during an experiment, control experiments were performed in which no electric field was applied. The intensity of the measurement beam was then adjusted to maximize sensitivity without photobleaching over the time scale of the experiment (≤10 s). Intensity versus time curves were obtained for 97 independent experiments. Curves selected for presentation in Figs. 2–4 are representative results.

Over the 0.02–10 s time scale of the experiment, single electroporation pulses (1.0–3.8 kV/cm in strength) caused extensive efflux of calcein across erythrocyte ghost membranes. Ghosts were partially (Fig. 2 *A*) or fully (Fig. 2 *B*) emptied of calcein. Although some ghosts were only partially emptied, additional transport could have occurred after the conclusion of the experiment, resulting in complete emptying over a longer time scale. However, in most experiments, efflux appeared to stop within the time scale of data collection.

Measurements with millisecond temporal resolution were used to distinguish between efflux during and after the electroporation pulse. One of four kinetic profiles was typically observed. Ghosts were (1) partially emptied of calcein, involving efflux primarily after the pulse (Fig. 3, *A* and *B*); (2) completely emptied of calcein, involving efflux primarily after the pulse (Fig. 3, *C* and *D*); (3) completely emptied of calcein, involving efflux both during and after the pulse (Fig. 3, *E* and *F*); or (4) completely emptied of calcein, involving efflux primarily during the pulse (Fig. 3, *G* and *H*). Partial emptying, involving significant efflux during the pulse, was generally not observed. In cases for which efflux occurred largely during the pulse, transport kinetics were also analyzed with data collected at 200-μs intervals (Fig. 4).

Data from 97 such electroporation experiments were pooled and analyzed. As shown in Fig. 5, significant efflux occurred both during and after a pulse. Both the total amount of calcein efflux and the fraction of calcein released during the electroporation pulse correlated with the electric field strength. Overall, post-pulse efflux accounted for 30–75% of the total efflux that occurred over the time scale of the experiment (Fig. 5, Table 1).

DISCUSSION

Electrical (Coster and Zimmermann, 1975; Kinosita and Tsong, 1977b; O'Neill and Tung, 1991) and optical (Hibino et al., 1991; Neumann et al., 1992) techniques have been used to assess membrane structural changes caused by electroporation with sub-millisecond time resolution. However, measurements of the molecular transport associated with these changes have not been performed on time scales equal to or faster than the applied pulse length, making separate assessment of transport during and after the pulse difficult. The fastest electroporation transport measurements known to us were performed with 17-ms time resolution (Dimitrov and Sowers, 1990). Here, data have been collected over time intervals as short as 0.2 ms.

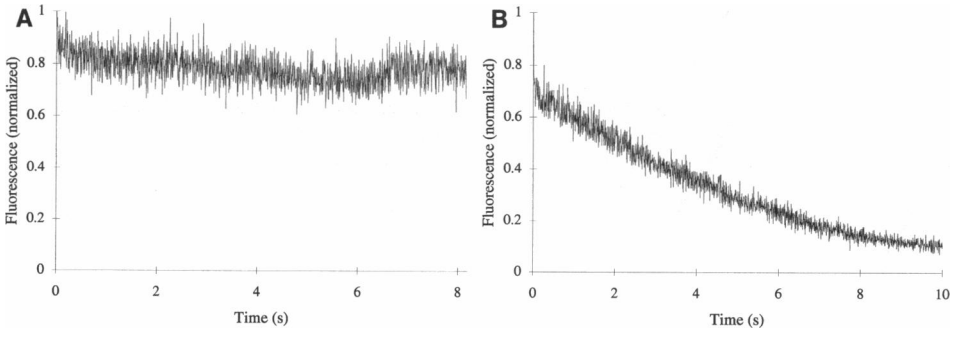

FIGURE 2 Normalized fluorescence of individual calcein-loaded erythrocyte ghosts during and after single exponential decay electric field pulses (5-ms resolution). Calcein is a small, fluorescent molecule that is unable to cross erythrocyte ghost membranes resealed after hemolysis. Fluorescence values are normalized to prepulse values. (*A*) Approximately 25% of the calcein was transported out of the ghost over the time scale of the experiment. Nominal electric field strength, E = 1.0 kV/cm; exponential decay time constant of pulse, τ = 2.3 ms. (*B*) At least 90% of the calcein was transported out of the ghost over the time scale of the experiment. E = 1.5 kV/cm, τ = 2.7 ms.

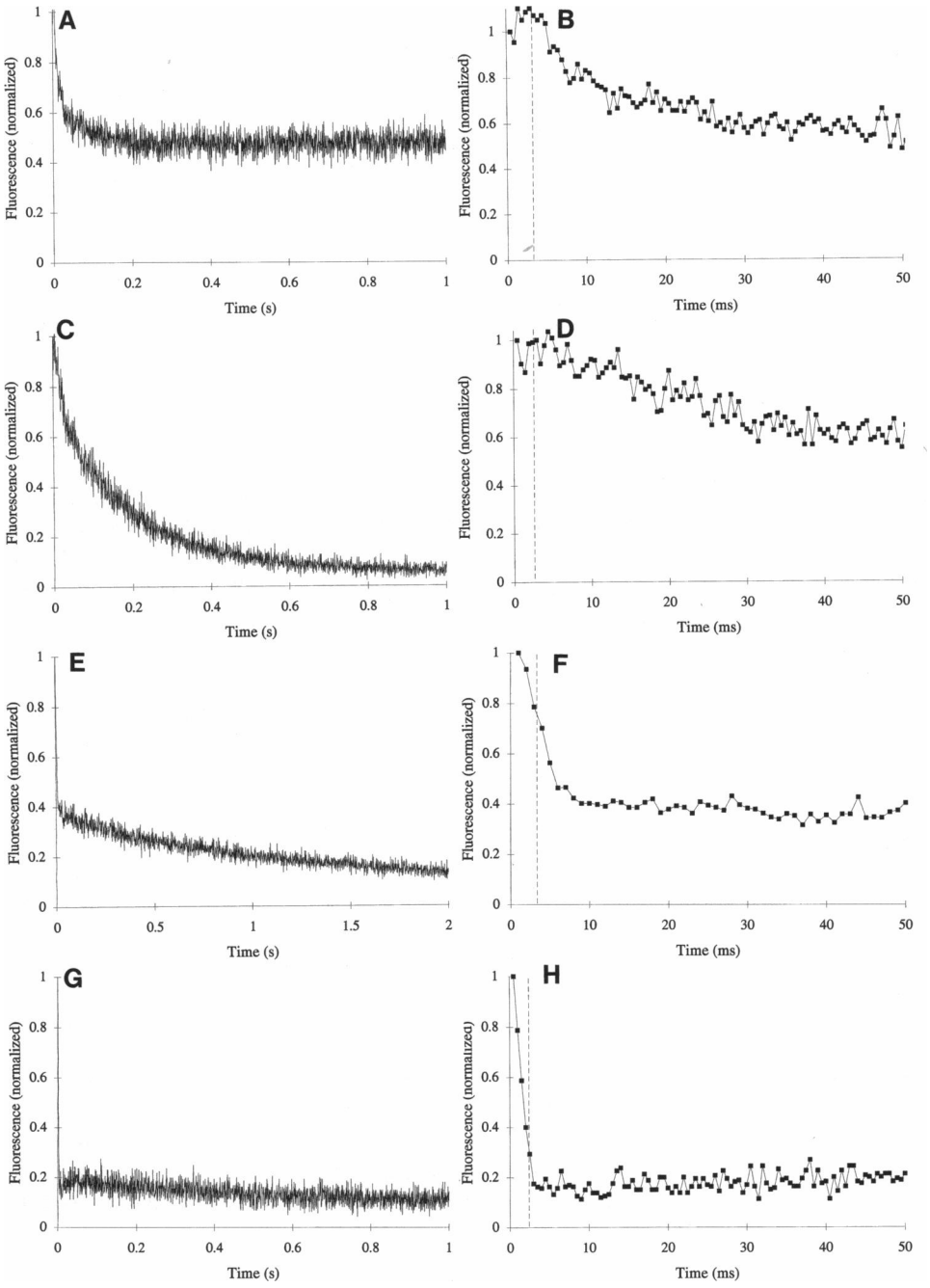

FIGURE 3 Normalized fluorescence of individual calcein-loaded erythrocyte ghosts during and after single exponential decay electric field pulses (0.5–1 ms resolution). (*A* and *B*) The ghost was only partially emptied of calcein; most efflux occurred after the pulse. E = 2.5 kV/cm; τ = 3.4 ms. (*C* and *D*) The ghost was completely emptied of calcein; most efflux occurred after the pulse. E = 2.5 kV/cm; τ = 2.6 ms. (*E* and *F*) The ghost was completely emptied of calcein; extensive efflux occurred both during and after the pulse. E = 2.5 kV/cm; τ = 3.4 ms. (*G* and *H*) The ghost was completely emptied of calcein; most efflux occurred during the pulse. E = 2.5 kV/cm; τ = 2.4 ms. Each pair of graphs (e.g., *A* and *B*) contains the same data shown on different time scales. The dashed lines indicate the time constant, τ, of the pulse.

Previous studies of electroporation transport kinetics have often used molecules that fluoresce upon binding to a substrate (e.g., ethidium bromide binding to DNA) (Marszalek et al., 1990; Tekle et al., 1991; Sixou and Teissié, 1993). Such measurements, of necessity, couple transport and binding rates. In contrast, the calcein fluorescence measured here should be directly related to transport kinetics and independent of any binding rate.

Mechanisms of transport

We consider the mechanisms by which efflux could occur during and after an electroporation pulse. During a pulse, efflux could occur through electropores by diffusion and/or electrically driven transport, such as electroosmosis and electrical drift. To compare the relative importance of diffusion with electroosmosis, we calculate a Peclet number, Pe, which is the ratio of the characteristic times of diffusion and electroosmotic convection:

$$Pe = \frac{ur}{D}$$

$$u = \mu E$$

where u is electroosmotic velocity, r is ghost radius (4×10^{-4} cm (Prausnitz et al., 1993)), D is calcein diffusivity ($3.5 \times$

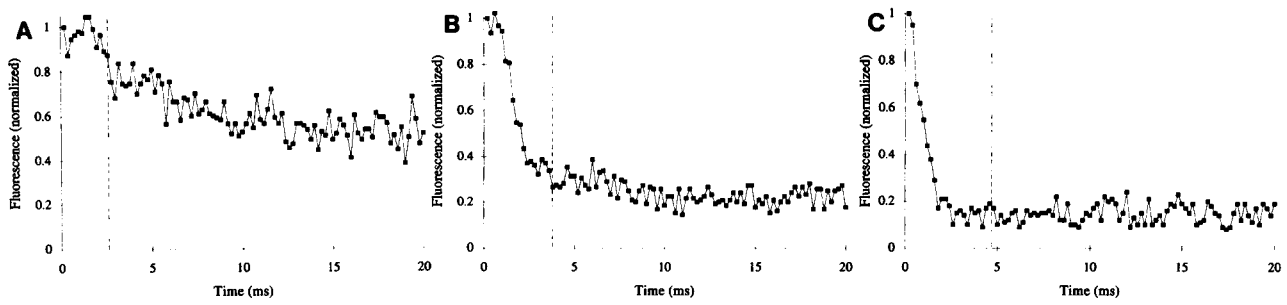

FIGURE 4 Normalized fluorescence of individual calcein-loaded erythrocyte ghosts during and after single exponential decay electric field pulses (200-μs resolution). (*A*) Most efflux occurred on a time scale on the order of 10 ms. E = 2.5 kV/cm; τ = 2.6 ms. (*B*) Most efflux occurred on a time scale on the order of 1 ms. E = 3.8 kV/cm; τ = 3.8 ms. (*C*) Most efflux occurred on a time scale on the order of 1 ms. E = 3.8 kV/cm; τ = 4.7 ms. The dashed lines indicate the time constant, τ, of the pulse.

10^{-6} cm^2/s (M. R. Prausnitz, C. S. Lee, C. H. Liu, J. C. Pang, T.-P. Singh, R. Langer, and J. C. Weaver. Transdermal transport efficiency during skin electroporation, and iontophoresis. Submitted for publication)), μ is electrophoretic velocity of the mobile cations, assumed to be sodium (5×10^{-4} cm^2/V s (Atkins, 1986)), and E is electric field strength (2.5 kV/cm, as a representative value).

To compare diffusion with electrical drift, we define a modified Peclet number, Pe*, which has the same form as Pe, except that the electrophoretic velocity of calcein, u*, is used instead of the electroosmotic velocity, u. u* is calculated by using the electrophoretic mobility of calcein, μ*(-6×10^{-4} cm^2/V s (Prausnitz et al., submitted for publication)). With the values given above, Pe = 143 and Pe* = 171. Such large Peclet numbers indicate that, during a pulse, electrically driven efflux, by either electroosmosis or electrical drift, is much faster than diffusion. This finding is in agreement with previous calculations (Dimitrov and Sowers, 1990; Weaver and Barnett, 1992).

In contrast, after a pulse, no electric fields are applied and efflux is expected to occur only by diffusion through long-lived reversible or irreversible pores. Low voltage electrically driven transport caused by a small transmembrane diffusion potential has also been proposed (Weaver and Barnett, 1992). However, with the exception of calcein, the composition of solutes inside and outside the ghosts used here was the same, making diffusion potentials unlikely.

The analysis presented above suggests that, when ghosts are completely emptied of calcein during the pulse (e.g., see Fig. 3, *G* and *H*), efflux is driven predominantly by electrophoresis and/or electroosmosis. This interpretation is in agreement with previous studies (Dimitrov and Sowers, 1990; Klenchin et al., 1991; Weaver and Barnett, 1992; Orlowski and Mir, 1993; Prausnitz et al., 1994). However, when significant efflux occurs after the pulse (e.g., see Fig. 3, *A–F*), transport must occur in part or almost completely by diffusion. Although rates of electrically driven efflux are generally faster than diffusion, electrophoresis and electroosmosis occur only for the duration of a pulse (milliseconds) whereas transmembrane diffusion occurs for orders of magnitude longer (i.e., as long as pores exist). Thus, the net time-integrated contribution of diffusion is often greater than that of electrically driven transport. In this study, efflux by diffusion after a pulse may have been facilitated by the relatively small size of calcein (Stokes-Einstein radius, r = 0.6 nm (Edwards et al., in press)). In contrast, the contribution of post-pulse diffusion of macromolecules, such as proteins or DNA, may be significantly smaller, as long-lived elec-

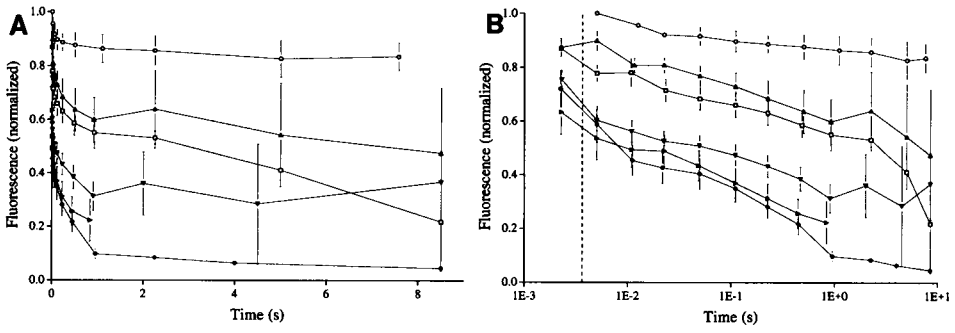

FIGURE 5 Average normalized fluorescence of individual calcein-loaded erythrocyte ghosts during and after single exponential decay electric field pulses. E = 1.0 kV/cm (○), 1.5 kV/cm (△), 1.9 kV/cm (□), 2.5 kV/cm (▽), 3.1 kV/cm (◇), 3.8 kV/cm (▷); τ = 3.6 ± 1.1 ms (mean ± standard deviation). *A* and *B* contain the same data, presented on different time axes. This figure contains data from 97 independent electroporation experiments like those shown in Figs. 2–4. Each point represents the average normalized fluorescence of ghosts from 2–40 different experiments. Standard error bars are shown. The dashed line indicates the average time constant, τ, of the pulse.

TABLE 1 Calcein efflux across erythrocyte ghost membranes during and after an electroporation pulse

Nominal field strength (kV/cm)	Fraction released during pulse	Total fraction released	Ratio (during/total)
1.0	0.04	0.16	0.25
1.5	0.19	0.52	0.37
1.9	0.22	0.78	0.28
2.5	0.44	0.63	0.70
3.1	0.54	0.95	0.57
3.8	0.50		

With data from Fig. 5, the fraction of calcein transported out of the ghost during the pulse and the total fraction transported over the time scale of the experiment are shown. Efflux during the pulse corresponds to the amount transported within the first 10 ms of the exponential decay pulse (approximately three time constants). Total efflux represents calcein transported within approximately 8 s (data for 3.8-kV/cm pulses were not collected over a time scale long enough to calculate total efflux). These data suggest that, although efflux generally occurred during the pulse, significant efflux also occurred after the pulse, probably by passive diffusion through long-lived and/or irreversible pores.

tropores are thought to be ~1 nm in radius (Abidor et al., 1979; Glaser et al., 1988b).

Previous studies have suggested that most transport caused by electroporation occurs during the pulse and is electrically driven (Taketo, 1988; Dimitrov and Sowers, 1990; Klenchin et al., 1991). This conclusion is based largely on experiments in which the molecules to be transported were added to cell suspensions either before or seconds to minutes after pulsing (Taketo, 1988; Klenchin et al., 1991; Chang et al., 1992). Since much more transport was generally observed when molecules were added before, one might conclude that most transport occurred during the pulse. However, a more precise conclusion is that most transport occurred during and/or within seconds to minutes after the pulse.

Data presented here were collected on time scales sufficiently rapid to distinguish between transport during and immediately after a pulse. This is important, because post-pulse diffusion may often occur predominantly within a few seconds after the pulse; e.g., significant efflux by post-pulse diffusion was observed here on the millisecond to second time scale (Figs. 2–3) and pore closure kinetics have also been observed on the millisecond to second time scale (Zimmermann et al., 1975; Chernomordik et al., 1987; Chang and Reese, 1990; Hibino et al., 1991; Zhelev and Needham, 1993). Our results suggest that, under some circumstances, transport by post-pulse diffusion within seconds after the pulse can make an equal or greater contribution to net transport than electrically driven transport during the pulse. This conclusion could not have been reached on the basis of previous experiments, in which transport during and immediately after the pulse could not be separately assessed.

In agreement with results reported here, kinetic studies have suggested that rates of transport are greater during a pulse than after (Dimitrov and Sowers, 1990; Sixou and Teissié, 1993). Moreover, studies that indicate that transport occurs predominantly in a single direction oriented parallel to the applied electric field suggest that transport during a pulse is primarily driven by electrophoresis (Klenchin et al., 1991) and/or electroosmosis (Dimitrov and Sowers, 1990). However, given the vastly different time scales over which diffusion and electrically driven transport occur, these observations do not exclude a significant contribution of diffusion to net transport under all conditions.

In summary, we conclude that, in some cases, transport caused by electroporation is predominantly electrically driven, in agreement with others. However, we find that, in other cases, transport can occur in part or almost completely by diffusion within seconds after a pulse.

Functional dependence of transport kinetics

The functional dependence of rates of efflux gives additional insight into transport mechanisms and electropore closure kinetics. Fig. 5 *B* suggests a reasonable correlation for a logarithmic dependence of calcein concentration on time ($C \sim \log t$; $r^2 = 0.93 \pm 0.04$, mean correlation constant ± standard deviation). A reasonable fit for a power function dependence was also found ($C \sim t^a$; $0.02 < a < 0.34$; $r^2 = 0.90 \pm 0.08$). However, no mechanistic basis for these correlations is evident.

One-dimensional transport by electrical drift is predicted to be proportional to the electric field strength (Bockris and Reddy, 1970). However, correlations here were poor for both an exponential decay ($C \sim e^{-t}$; $r^2 = 0.65 \pm 0.22$), corresponding to the bulk electric field, and a linear fit ($C \sim t$, $r^2 = 0.55 \pm 0.20$), corresponding to the local electric field within electropores (Freeman et al., 1994). For one-dimensional diffusion from a point source, which is expected to show a linear dependence of concentration on the inverse of the square root of time (Crank, 1975), the data correlated better ($C \sim t^{-1/2}$; $r^2 = 0.80 \pm 0.13$). For one-dimensional diffusion from a source of finite thickness, which more closely describes the true geometry, a linear correlation with the error function is expected (Crank, 1975),

$$C = erf\left(\frac{r}{2\sqrt{Dt}}\right)$$

where C is the normalized calcein concentration at the center of the ghost, r is ghost radius (4×10^{-4} cm (Prausnitz et al., 1993)), D is calcein diffusivity (3.5×10^{-6} cm^2/s (Prausnitz et al., submitted for publication)) and t is time. In this case, the correlation was better ($r^2 = 0.89 \pm 0.08$), and deviation from linearity was primarily observed at short times (i.e., during the pulse).

Although the simple model of diffusion from a source of finite thickness provides a reasonable correlation, diffusion from concentric spheres having different diffusivities (representing the ghost membrane and interior) could be used to more fully delineate the physics of the electroporation problem. For time-independent diffusivities, the solution takes the form of an infinite sum of exponentials ($C = \Sigma e^{-t}$) (Bell, 1945). However, to reflect the time-dependent nature of electropores, the derivation would need to be modified to include an outer sphere (representing the ghost membrane) with

time-dependent diffusivity. Electrically driven transport during a pulse would also have to be included. Analysis at this level of complexity is beyond the scope of the present study.

We thank C. D. Milano for assistance in preparing erythrocyte ghosts, U. Pliquett for help with data analysis, T. E. Vaughan for electric field validation, and V. G. Bose, E. A. Gift, H. S. Thatte, and A. E. Sowers for helpful advice.

This work was supported in part by Cygnus Therapeutic Systems (M.R.P., J.C.W.), National Institutes of Health Training grant HL07623 (J.D.C.), ARO grant DAAL03-90-G-0218 (J.C.W.), and National Institutes of Health grants HL15157 (D.E.G.), HL32854 (D.E.G.), GM44884 (R.L.), and GM34077 (J.C.W.).

REFERENCES

Abidor, I. G., V. B. Arakelyan, L. V. Chernomordik, Y. A. Chizmadzhev, V. F. Pastushenko, and M. R. Tarasevich. 1979. Electric breakdown of bilayer membranes: I. The main experimental facts and their qualitative discussion. *Bioelectrochem. Bioenerget.* 6:37–52.

Atkins, P. W. 1986. Physical Chemistry. W. H. Freeman and Co., New York.

Barnett, A., and J. C. Weaver. 1991. A unified, quantitative theory of reversible electrical breakdown and rupture. *Bioelectrochem. Bioenerget.* 25:163–182.

Bell, R. P. 1945. A problem of heat conduction with spherical symmetry. *Proc. Phys. Soc. (Lond.)* 57:45–48.

Benz, R. F., F. Beckers, and U. Zimmermann. 1979. Reversible electrical breakdown of lipid bilayer membranes: a charge-pulse relaxation study. *J. Membr. Biol.* 48:181–204.

Bockris, J. O., and A. K. N. Reddy. 1970. Modern Electrochemistry. Plenum, New York.

Chang, D. C., B. M. Chassy, J. A. Saunders, and A. E. Sowers, editors. 1992. Guide to Electroporation and Electrofusion. Academic Press, New York.

Chang, D. C., and T. S. Reese. 1990. Changes in membrane structure induced by electroporation as revealed by rapid-freezing electron microscopy. *Biophys. J.* 58:1–12.

Chernomordik, L. V., S. I. Sukharev, I. G. Abidor, and Y. A. Chizmadzhev. 1983. Breakdown of lipid bilayer membranes in an electric field. *Biochim. Biophys. Acta.* 736:203–213.

Chernomordik, L. V., S. I. Sukharev, S. V. Popov, V. F. Pastushenko, A. V. Sokirko, I. G. Abidor, and Y. A. Chizmadzhev. 1987. The electrical breakdown of cell and lipid membranes: the similarity of phenomenologies. *Biochim. Biophys. Acta.* 902:360–373.

Corbett, J. D., and D. E. Golan. 1993. Band 3 and glycophorin are progressively aggregated in density-fractionated sickle and normal red blood cells: evidence from rotational and lateral mobility studies. *J. Clin. Invest.* 91:208–217.

Coster, H. G. L., and U. Zimmermann. 1975. The mechanism of electrical breakdown in the membranes of *Valonia utricularis*. *J. Membr. Biol.* 22:73–90.

Crank, J. 1975. The Mathematics of Diffusion. Clarendon Press, Oxford.

Dimitrov, D. S., and A. E. Sowers. 1990. Membrane electroporation–fast molecular exchange by electroosmosis. *Biochim. Biophys. Acta.* 1022: 381–392.

Edwards, D. A., M. R. Prausnitz, R. Langer, and J. C. Weaver. 1995. Analysis of enhanced transdermal transport by skin electroporation. *J. Controlled Release.* In press.

Freeman, S. A., M. A. Wang, and J. C. Weaver. 1994. Theory of electroporation of planar membranes: predictions of the aqueous area, change in capacitance and pore-pore separation. *Biophys. J.* 67:42–56.

Glaser, R. W., S. L. Leikin, L. V. Chernomordik, V. F. Pastushenko, and A. I. Sokirko. 1988. Reversible electrical breakdown of lipid bilayers: formation and evolution of pores. *Biochim. Biophys. Acta.* 940:275–287.

Hibino, M., M. Shigemori, H. Itoh, K. Nagayama, and K. Kinosita. 1991. Membrane conductance of an electroporated cell analyzed by submicrosecond imaging of transmembrane potential. *Biophys. J.* 59:209–220.

Kinosita, K., and T. Y. Tsong. 1977a. Formation and resealing of pores of controlled sizes in human erythrocyte membrane. *Nature.* 268:438–441.

Kinosita, K., and T. Y. Tsong. 1977b. Voltage-induced pore formation and hemolysis of human erythrocytes. *Biochim. Biophys. Acta.* 471:227–242.

Klenchin, V. A., S. I. Sukharev, S. M. Serov, L. V. Chernomordik, and Y. A. Chizmadzhev. 1991. Electrically induced DNA uptake by cells is a fast process involving DNA electrophoresis. *Biophys. J.* 60:804–811.

Lambert, H., R. Pankov, J. Gauthier, and R. Hancock. 1990. Electroporation-mediated uptake of proteins into mammalian cells. *Biochem. Cell Biol.* 68:729–734.

Lee, R. C., L. P. River, F. Pan, L. Ji, and R. L. Wollmann. 1992. Surfactant induced sealing of electropermeabilized skeletal muscle membranes in vivo. *Proc. Natl. Acad. Sci. USA.* 89:4524–4528.

Marszalek, P., D.-S. Liu, and T. Y. Tsong. 1990. Schwan equation and transmembrane potential induced by alternating electric field. *Biophys. J.* 58:1053–1058.

Mishra, K. P., and B. B. Singh. 1986. Temperature effects on resealing of electrically hemolysed rabbit erythrocytes. *Indian J. Exp. Biol.* 24: 737–741.

Neumann, E., A. E. Sowers, and C. A. Jordan. 1989. Electroporation and Electrofusion in Cell Biology. Plenum Press, New York.

Neumann, E., E. Werner, A. Sprafke, and K. Kruger. 1992. Electroporation phenomena. Electrooptics of plasmid DNA and of lipid bilayer vesicles. *In* Colloid and Molecular Electro-Optics 1992. B. R. Jennings and S. P. Stoylov, editors. IOP Publishing, Bristol. pp. 197–206.

O'Neill, R. J., and L. Tung. 1991. Cell-attached patch clamp study of the electropermeabilization of amphibian cardiac cells. *Biophys. J.* 59: 1028–1039.

Orlowski, S., and L. M. Mir. 1993. Cell electropermeabilization: a new tool for biochemical and pharmacological studies. *Biochim. Biophys. Acta.* 1154:51–63.

Prausnitz, M. R., B. S. Lau, C. D. Milano, S. Conner, R. Langer, and J. C. Weaver. 1993. A quantitative study of electroporation showing a plateau in net molecular transport. *Biophys. J.* 65:414–422.

Prausnitz, M. R., C. D. Milano, J. A. Gimm, R. Langer, and J. C. Weaver. 1994. Quantitative study of molecular transport due to electroporation: uptake of bovine serum albumin by erythrocyte ghosts. *Biophys. J.* 66:1522–1530.

Rols, M.-P., and J. Teissié. 1990. Electropermeabilization of mammalian cells: quantitative analysis of the phenomenon. *Biophys. J.* 58: 1089–1098.

Sale, A. J. H., and W. A. Hamilton. 1968. Effects of high electric fields on microorganisms. III. Lysis of erythrocytes and protoplasts. *Biochim. Biophys. Acta.* 163:37–43.

Sixou, S., and J. Teissié. 1993. Exogenous uptake and release of molecules by electroloaded cells: a digitized videomicroscopy study. *Bioelectrochem. Bioenerget.* 31:237–257.

Taketo, A. 1988. DNA transfection of *Escherichia coli* by electroporation. *Biochim. Biophys. Acta.* 949:318–324.

Tekle, E., R. D. Astumian, and P. B. Chock. 1991. Electroporation by using bipolar oscillating electric field: an improved method for DNA transfection of NIH 3T3 cells. *Proc. Natl. Acad. Sci. USA.* 88:4230–4234.

Tsong, T. Y. 1991. Electroporation of cell membranes. *Biophys. J.* 60: 297–306.

Weaver, J. C. 1993. Electroporation: a general phenomenon for manipulating cells and tissues. *J. Cell. Biochem.* 51:426–435.

Weaver, J. C., and A. Barnett. 1992. Progress towards a theoretical model for electroporation mechanism: membrane electrical behavior and molecular transport. *In* Guide to Electroporation and Electrofusion. D. C. Chang, B. M. Chassy, J. A. Saunders and A. E. Sowers, editors. Academic Press, New York. pp. 91–118.

Zhelev, D. V., and D. Needham. 1993. Tension-stabilized pores in giant vesicles: determination of pore size and pore line tension. *Biochim. Biophys. Acta.* 1147:89–104.

Zimmermann, U., G. Pilwat, and F. Riemann. 1975. Preparation of erythrocyte ghosts by dielectric breakdown of the cell membrane. *Biochim. Biophys. Acta.* 375:209–219.

Zimmermann, U., F. Riekmann, and G. Pilwat. 1976. Enzyme loading of electrically homogeneous human red blood cell ghosts prepared by dielectric breakdown. *Biochim. Biophys. Acta.* 436:460–474.